

Determining surface orientations of transparent objects based on polarization degrees in visible and infrared wavelengths

Daisuke Miyazaki

Institute of Industrial Science, The University of Tokyo, Tokyo 153-8505, Japan

Megumi Saito

Hewlett-Packard Japan, Ltd., Tokyo 168-8585, Japan

Yoichi Sato and Katsushi Ikeuchi

Institute of Industrial Science, The University of Tokyo, Tokyo 153-8505, Japan

Received May 15, 2001; revised manuscript received August 27, 2001; accepted October 3, 2001

Techniques for modeling an object through observation are very important in object recognition and virtual reality. A wide variety of techniques have been developed for modeling objects with opaque surfaces, whereas less attention has been paid to objects with transparent surfaces. A transparent surface has only surface reflection; it has little body reflection. We present a new method for obtaining surface orientations of transparent surfaces through analysis of the degree of polarization in surface reflection and emission in visible and far-infrared wavelengths, respectively. This parameter, the polarization degree of reflected light at the visible wavelengths, is used for determining the surface orientation at a surface point. The polarization degree at visible wavelengths provides two possible solutions, and the proposed method uses the polarization degree at far-infrared wavelengths to resolve this ambiguity. © 2002 Optical Society of America

OCIS codes: 110.3080, 110.6880, 120.4630, 120.6650, 260.5430, 330.7310.

1. INTRODUCTION

Recently techniques for modeling objects through observation have been extensively investigated. Such modeling has a wide range of applications, including virtual reality and object recognition. Geometry, one of the most important aspects of modeling, can be used to create a model based on measuring the shape of an object.

Many techniques to measure object shape have been developed in the field of optical engineering. These techniques can be classified into two categories: point type and surface type. A point-type method, such as a laser range sensor, measures object shape by projecting a spotlight, often a laser beam, over the object surface and measuring the returned timing or the returned direction. A surface method, such as moiré topography, determines the shape of an object by projecting a planar light and measuring the interference of the light with the surface.

The computer vision community has developed such techniques extensively. Shape from shading, for example, analyzes shading information in an image with a reflectance map to relate image brightness to surface orientations. The photometric stereo method obtains information from three images taken from the same position under three different illumination conditions. Binocular stereo and motion analysis techniques use differences in a series of images taken from different positions.

Most of these methods are, however, designed to obtain the shapes of opaque surfaces. That is, the techniques

are based on analysis of the body reflection component of an object surface. Models of transparent objects, which have only surface reflection, cannot be created by using these techniques. Few existing methods attempt to determine object shape through surface reflection.

With regard to surface reflection, Ikeuchi¹ proposed to determine the reflectance of a metal surface by using photometric stereo. When exposed to three different extended light sources, a metal surface generates different illumination distributions over the surface. The application of the photometric stereo method to these illumination distributions allows the shape of a metal surface to be determined. Nayar *et al.*² extended the method by using continuous illumination distribution, referred to as a photometric sampler. Their method determines not only surface shape but also surface reflectance parameters. Sato *et al.*³ analyzed color images in a similar setting and determined the shape and reflectance of shiny objects for computer graphics purposes. Oren and Nayar⁴ proposed a method using surface reflections and motion to determine surface shape.

Surface reflection can also be analyzed through the degree of polarization, as demonstrated by Koshikawa,⁵ who proposed to use the degree of polarization, employing polarized light sources, to determine the shape of metal surfaces. Later, Koshikawa and Shirai⁶ applied this method to the recognition of objects. Wolff⁷ proposed to analyze the degree of polarization in visible light for that same

purpose. Wolff *et al.*⁸ concluded that by analyzing the polarization of the object the surface normal of the object surface is constrained; Rahmann⁹ addressed the potential of recovering shape from polarization; and Jordan *et al.*^{10,11} and Wolff *et al.*¹² analyzed the degree of polarization at infrared wavelengths.

A transparent surface also has surface reflection components. Szeliski *et al.*¹³ analyzed the movement of surface reflection components on a transparent object and separated surface reflection from background images. Schechner *et al.*¹⁴ proposed a method with which to determine only the surface reflection component, using the degree of polarization. That method also addressed the extraction of information about the orientation of transparent planes. For graphics applications, Zongker *et al.*¹⁵ developed a method with which to generate the appearance of a transparent object from a series of images taken under different background conditions. These methods, however, do not provide shape information about a transparent object.

Saito *et al.*^{16,17} employed analysis of the degree of polarization and developed a method with which to measure the surface of a transparent object. Employing an extended light source originally developed by Nayar *et al.*,² they illuminated a transparent object and were able to obtain surface reflection components over the entire visible surface. Then, by measuring the degree of polarization, they determined surface orientations. Unfortunately, however, the method provides two solutions corresponding to one polarization degree. Thus the method can be applied to measuring a limited class of objects, or to surface inspection where rough surface orientation is predetermined; it cannot be applied to a general class of objects.

In this paper we propose to disambiguate these two solutions by introducing the degree of polarization in the infrared. This new method first obtains the degree of polarization at visible wavelengths, which was likewise obtained in Saito's method.^{16,17} One polarization degree measured corresponds to two surface orientations. The polarization degree in the infrared wavelength provides a single surface orientation to one polarization degree. Thus, by simultaneously measuring the degree of polarization in the infrared domain, we can uniquely determine the surface orientation. The measurement in the infrared domain cannot be used directly because the polarization ratio is relatively low in some areas; it is therefore better to use this measurement solely for judgment purposes.

In Section 2 we present the background theory of polarization and describe a method with which to obtain surface shape by using the polarization degrees at both visible and infrared wavelengths. In Section 3 we describe the apparatus of this method and the experimental results. Section 4 gives our conclusions.

2. POLARIZATION AND SHAPE DETERMINATION

A. Fresnel's Equation

The light that reflects at the surface of most types of objects can be separated into two major components, surface

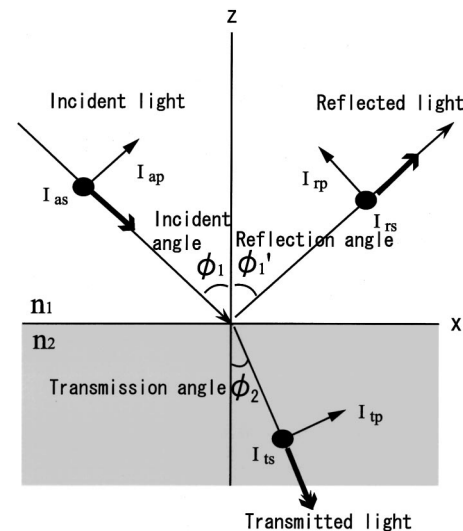


Fig. 1. Fresnel reflection.

reflection and body reflection. Incident light partly reflects at the surface and partly penetrates into the object. The light that penetrates into an opaque object randomly reflects at some of the pigments inside the object and is emitted into the air. The light that specularly reflects at the surface is called the surface reflection, and the light that is diffusely emitted into the air from inside the object is called the body reflection.¹⁸ We focus only on transparent objects in this paper, analyzing surface reflection rather than body reflection.

In this section, we will briefly overview the basic equation of reflection and refraction.¹⁹ In Fig. 1, let us consider the case in which a light hits the interface between two materials, the refractive indices of which are denoted n_1 and n_2 , respectively. Here we assume that the interface lies on the X–Y plane without loss of generality. One part of the light is reflected at the interface, while another part penetrates the interface and is refracted when entering the second material. Because we assume that both materials are transparent, we can neglect the component that is absorbed. We denote the incident, reflected, and refracted light by the subscripts a, r , and t , respectively, and identify the components parallel and perpendicular to the X–Y plane as p and s , respectively. The incident, reflecting, and transmitting angles are defined as ϕ_1 , ϕ_1' , and ϕ_2 , respectively, as shown in Fig. 1. Given that the incident and the reflected light pass through the same materials, $\phi_1 = \phi_1'$, we can define the parallel and perpendicular reflectance ratios, F_p and F_s , respectively, as

$$F_p = \frac{I_{rp}}{I_{ap}} = \frac{\tan^2(\phi_1 - \phi_2)}{\tan^2(\phi_1 + \phi_2)}$$

$$F_s = \frac{I_{rs}}{I_{as}} = \frac{\sin^2(\phi_1 - \phi_2)}{\sin^2(\phi_1 + \phi_2)}, \quad (1)$$

where I_{ap} is the intensity of the component of the incident light parallel to the X–Z plane, and I_{rp} is that of the reflected light. I_{as} is the intensity of the component of the incident light perpendicular to the X–Z plane, and I_{rs} is that of the reflected light. From Eq. (1), an incident angle to make $F_p = 0$ can be obtained. This incident

angle is referred to as the Brewster angle, ϕ_B . The Brewster angle is obtained by substituting $\phi_1 + \phi_2 = \pi/2$ (that is, $F_p = 0$) into Snell's equation, $n_1 \sin \phi_1 = n_2 \sin \phi_2$, as

$$\tan \phi_B = n_2/n_1. \tag{2}$$

B. Determining Surface Orientations by Using Polarization

The interface of a transparent object causes little diffuse reflection or absorption: under the condition of reflected light, the incident and reflecting angles are the same. Thus once the reflecting angle and the orientation of the plane of incidence are known, we can determine the surface orientation with respect to the viewer, as shown in Fig. 2. Here the plane of incidence is the one in which the light source, surface normal, and the viewer vectors lie. We will denote the direction of the plane of incidence and the reflecting angle θ and ϕ , respectively. We will determine these two angles by using the degree of polarization of the reflected light.

Generally, natural light is unpolarized; it oscillates in all directions in the plane of oscillation, which is perpendicular to the path of the light. Natural light, however, becomes polarized once it goes through a polarization material or is reflected from a surface. We will measure the degree of polarization in the latter case.

As shown in Eq. (1), the intensity of the reflected light varies depending on the direction of oscillation in the plane of oscillation; therefore a difference can be observed when the polarization filter is rotated in front of a CCD camera. The variance is described as a sinusoidal function of rotation angles. We will denote the maximum and minimum brightness in the observed intensities as I_{\max} and I_{\min} . Given that the sum of the maximum and minimum brightness is the total brightness of the reflected light, I_{spec} ,

$$I_{\max} = \frac{F_s}{F_p + F_s} I_{\text{spec}}, \quad I_{\min} = \frac{F_p}{F_p + F_s} I_{\text{spec}}. \tag{3}$$

By this equation, the direction parallel to the plane of incidence provides the minimum brightness I_{\min} . That is, by measuring the angle to give the minimum brightness,

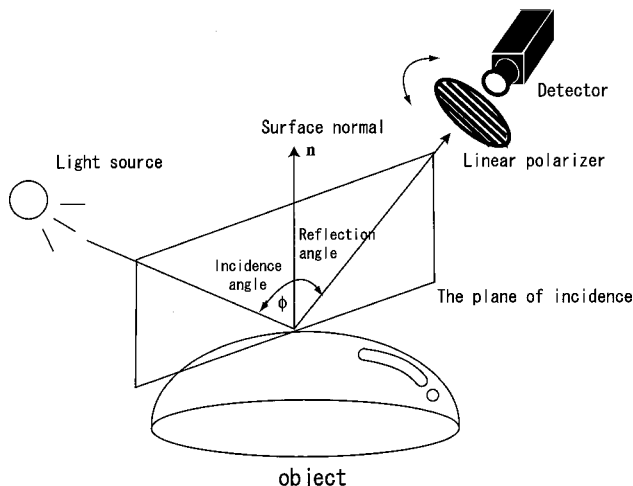


Fig. 2. Surface normal of object.

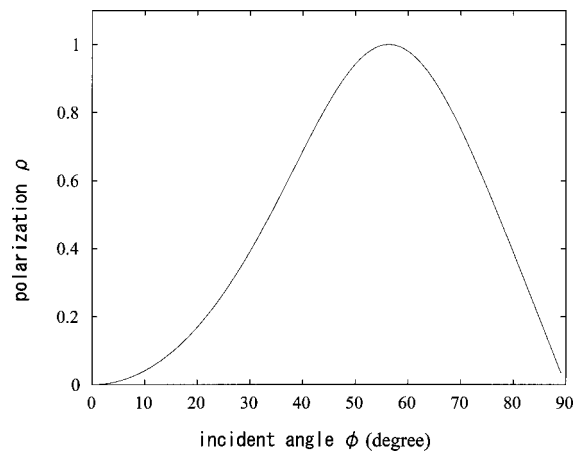


Fig. 3. Relation between the degree of polarization and the incident angle ($n = 1.5$).

we can determine the direction θ of the plane of incidence. There are two possible directions of the plane of incidence, θ_1 and θ_2 , which are definable as $\theta_2 = \theta_1 + \pi$. We assume the surface to have a convex shape, and we avoid this ambiguity.

The definition of the degree of polarization is as follows:

$$\rho = \frac{I_{\max} - I_{\min}}{I_{\max} + I_{\min}}. \tag{4}$$

The degree of polarization is 0 when the light is unpolarized, whereas it is 1 when the light is linearly polarized. The linearly polarized light is observed when the parallel component becomes 0. This occurs when the incident angle and the reflecting angle are at the Brewster angle.

By substituting Eqs. (3) and (1) into Eq. (4) along with Snell's law, we can represent the degree of polarization ρ as

$$\rho = \frac{2 \sin \phi \tan \phi \sqrt{n^2 - \sin^2 \phi}}{n^2 - \sin^2 \phi + \sin^2 \phi \tan^2 \phi}. \tag{5}$$

The degree of polarization is a function of the refractive index n and the incident angle ϕ . Thus by obtaining the degree of polarization from the data, we can determine the incident angle ϕ given the refractive index n .

Figure 3 shows the relation between the degree of polarization and the incident angle. Here the horizontal and vertical axes denote the incident angle and the degree of polarization, respectively. We can obtain the incident angle from the observed degree of polarization even if we do not know the intensity of the light source. The function has an extreme at the Brewster angle. From this function, an observed degree of polarization provides two possible incident angles, except at the Brewster angle. It is necessary to have a method to resolve this ambiguity. In this paper, we propose to solve this problem by considering the polarization of far-infrared light.

C. Thermal Radiation

Heat energy can propagate through space and is called heat propagation. A blackbody can completely absorb the heat energy radiated. According to Kirchoff's law,

the ratio between radiant and incoming heat energy is independent of the object and is dependent only on the temperature of the object. A blackbody, which completely absorbs energy, can also radiate more energy than any other objects at the same temperature.

From the Stephan–Boltzmann law, radiation energy W from the blackbody at the temperature T is

$$W = \sigma T^4, \quad (6)$$

where σ is the Stephan–Boltzmann coefficient and $\sigma = 5.67 \exp(-8)[\text{W}/\text{m}^2 \text{K}^4]$. Given that any object has a positive Kelvin temperature, it will radiate energy.

A blackbody has an energy distribution as shown in Fig. 4. From the figure it is apparent that the extremes of distributions shift along the temperature increment, and in the area of room temperature they exist in the infrared region. Thus it is appropriate to employ infrared measurement for measuring the radiation energy of an object at room temperature.

In Subsections 2.D and 2.E, we will derive the polarization degree in infrared light with two respective approaches. In Subsection 2.D the polarization degree is derived by using Kirchhoff's law, and in Subsection 2.E the polarization degree is derived by considering the light emitted from inside the object. As a result, both of the derived polarization degrees will be the same equation.

Glass is usually transparent in visible light, though it is somewhat translucent (or perhaps opaque?) in infrared light; that is, glass is more likely to absorb infrared light than visible light. First we will describe the unified theory of polarization in infrared light, which does not depend on whether the object is transparent, translucent, or opaque.

To actualize this concept, let us assume that in a sense all objects can be considered opaque; the light that hits the interface of objects can only reflect or be absorbed. The light that is transmitted into a transparent object will then be called the light that is absorbed into it. The light transmitted into a transparent object escapes into

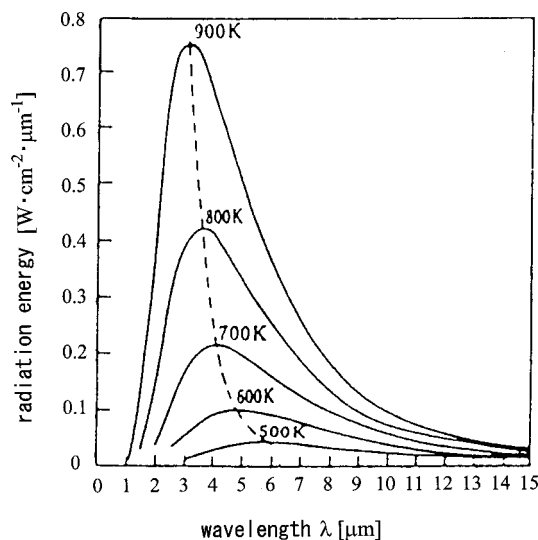


Fig. 4. Energy distribution of a blackbody.

the air somewhere from the surface of the object. Let us say that such escaped light is the light (thermally) emitted from the object.

This assumption that all objects can be considered opaque is used in Subsection 2.D. It holds when the system is in thermal equilibrium, given that all light is expected to have the same amount of energy and radiate in all directions.

D. Kirchhoff's Law

By considering the state in which the system is in thermal equilibrium, and by using Kirchhoff's law, we can explain the polarization of thermal radiation.^{10–12,20,21} A typical object emits an amount of radiation energy lower than that emitted from a blackbody, as noted above. The ratio of the amount of radiation energy from a typical object to that from a blackbody is referred to as the emissivity and is denoted ϵ .

Let us assume that infrared light strikes a smooth surface. Its components of intensity parallel and perpendicular to the plane of incidence are denoted as I_{ap} and I_{as} , respectively. When the infrared light strikes a surface with the incident angle ϕ , the intensity of parallel and perpendicular components of reflected light are given as $F_p I_{ap}$ and $F_s I_{as}$, respectively. These relationships were noted above in connection with Eq. (1).

From the law of the conservation of energy, the difference between the incoming and the reflected intensities, $(1 - F_p)I_{ap}$ and $(1 - F_s)I_{as}$, respectively, represents the amount of energy absorbed by the body. By denoting this ratio as absorptance α , and since Kirchhoff's law provides $\epsilon = \alpha$, we obtain

$$\begin{aligned} \epsilon_p(T, \lambda, \phi) &= 1 - F_p, \\ \epsilon_s(T, \lambda, \phi) &= 1 - F_s. \end{aligned} \quad (7)$$

Let us denote the intensity of thermal radiation from the blackbody by W . Then the intensity of thermal radiation from our object is ϵW , and its polarization can be written by using Eq. (7):

$$\begin{aligned} \rho_{\text{IR}} &= \frac{I_{\text{max}} - I_{\text{min}}}{I_{\text{max}} + I_{\text{min}}} = \frac{\epsilon_p W - \epsilon_s W}{\epsilon_p W + \epsilon_s W} \\ &= \frac{F_s - F_p}{2 - F_p - F_s}, \end{aligned} \quad (8)$$

where ρ_{IR} is the polarization degree in infrared light. We use the different notation to distinguish this condition from that for visible light. By substituting Eq. (1) for Eq. (8), we can derive the relation between the polarization ratio ρ_{IR} and the emitting angle ϕ .

E. Light Emitted from Inside the Object

We now explain the polarization phenomenon of thermal radiation by considering the light emitted from inside the object.²² Thermal radiation from inside the object is transmitted through the interface surface and radiated into the air.

Material 1 will be the object and material 2 will be the air, as shown in Fig. 1. In this case, $\phi_2 > \phi_1$. We denote the refractive index of material 1 as n_1 and that of material 2 as n_2 . Thus the refractive index of the object

relative to the air will be $n = n_1/n_2$. Angle ϕ_2 is the emitting angle, and we will derive the polarization degree as a function of $\phi = \phi_2$.

We can define the parallel and perpendicular intensity ratios of transmission, T_p and T_s , as

$$T_p = \frac{I_{tp}}{I_{ap}} = \frac{\sin 2\phi_1 \sin 2\phi_2}{\sin^2(\phi_1 + \phi_2) \cos^2(\phi_1 - \phi_2)},$$

$$T_s = \frac{I_{ts}}{I_{as}} = \frac{\sin 2\phi_1 \sin 2\phi_2}{\sin^2(\phi_1 + \phi_2)}, \quad (9)$$

where I_{tp} is the component parallel to the X-Z plane of the transmitting light, and I_{ts} is the component perpendicular to the X-Z plane of the transmitting light. Thus I_{\max} and I_{\min} will be written by using the total energy of the emitted light, W , as

$$I_{\max} = \frac{T_p}{T_p + T_s} W, \quad I_{\min} = \frac{T_s}{T_p + T_s} W. \quad (10)$$

By substituting Eqs. (10) and (9) into Eq. (4) along with Snell's law, we can represent the degree of polarization of thermal radiation ρ_{IR} as

$$\rho_{\text{IR}} = \frac{I_{\max} - I_{\min}}{I_{\max} + I_{\min}} = \frac{T_p - T_s}{T_p + T_s} = \frac{s}{2 - s},$$

$$s = \sin^2 \phi \left\{ 1 + \frac{1}{n^2} - \frac{2}{n^2} \sin^2 \phi - \frac{2}{n} \left[(1 - \sin^2 \phi) \left(1 - \frac{1}{n^2} \sin^2 \phi \right) \right]^{1/2} \right\}. \quad (11)$$

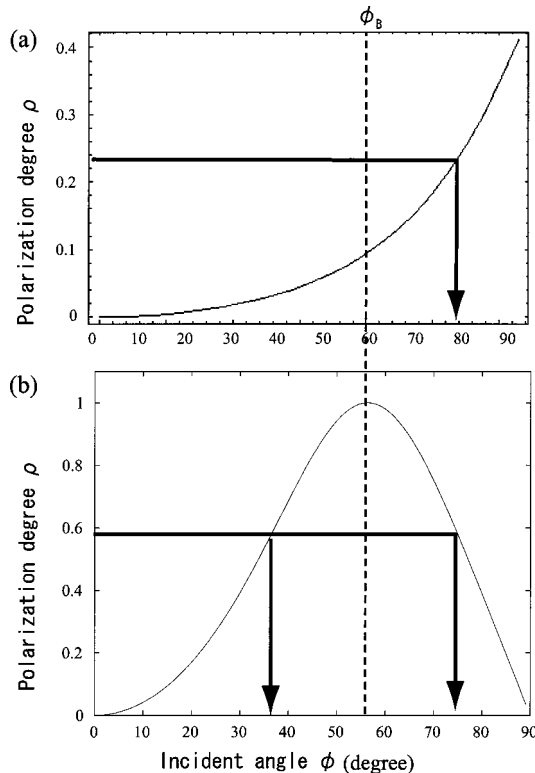


Fig. 5. Polarization degree of (a) infrared light ($n = 1.5$), (b) visible light ($n = 1.5$).

F. Graph of Polarization Degree in Infrared Light

$F_p + T_p = 1$ and $F_s + T_s = 1$ holds, and thus the resulting ρ_{IR} in Eqs. (8) and (11) are the same. This is because the two explanations deal with the same phenomenon, though the approach is different: One is based on the energy conservation law (Kirchhoff's law) and the other on the mechanism of the phenomenon.

Figure 5(a) shows the relation between the polarization ratio ρ_{IR} and the emitting angle ϕ .

The refractive index of the material represented by the graph shown in Fig. 5(a) is 1.5. Because the refractive index is affected by the wavelength, the refractive index of infrared light is slightly different from that of visible light. For example, the refractive index of glass is approximately 1.52 when the wavelength is approximately 500 nm (visible light), and the refractive index of glass is approximately 1.49 when the wavelength is approximately $2 \mu\text{m}$ (infrared light). We use the same refractive index in infrared light as in visible light because the difference is negligible.

As shown in Fig. 5(a), the relation is a one-valued function; there is a one-to-one correspondence between the polarization and the emitting angle. Thus once we measure the polarization ratio in infrared light, we can uniquely determine the emitting angle. For the sake of comparison, Fig. 5(b) represents the visible light condition. In this function, as mentioned, one polarization ratio corresponds to two emitting angles.

Unfortunately, however, the polarization ratio in emitted infrared light is much smaller than that in reflected visible light; at the maximum, near an emitting angle of 90 deg, it is only 40%. For lower angles of incidence, as shown in Fig. 5(a), the ratio is smaller than 10%. In order to obtain such a smaller ratio, we are required to measure I_{\max} and I_{\min} precisely. It is impractical to perform such a highly accurate measurement by using an ordinary CCD camera with a 256-gray level.

To overcome this difficulty, we propose to use both visible and infrared light. By using visible light, we can achieve a highly accurate measurement though with ambiguity. By using infrared light, we discriminate between the two sides. First we determine the polarization ratio in the infrared region at the Brewster angle. Using this ratio as the threshold value, we can determine on which side, with respect to the Brewster angle, the emitting angle falls, as indicated by the vertical dashed line in Fig. 5.

3. DETERMINING SURFACE ORIENTATION OF TRANSPARENT OBJECT

A. Apparatus for Visible Light Measurement

Figure 6(a) shows the apparatus for visible light measurement. As a light source, we employ a spherical diffuser illuminated from point light sources. This spherical diffuser becomes a secondary light source and illuminates an object that is located at the center of the sphere from all directions. Because we determine surface orientations using only surface reflection and the surface reflection occurs only when the emitting and incident angles

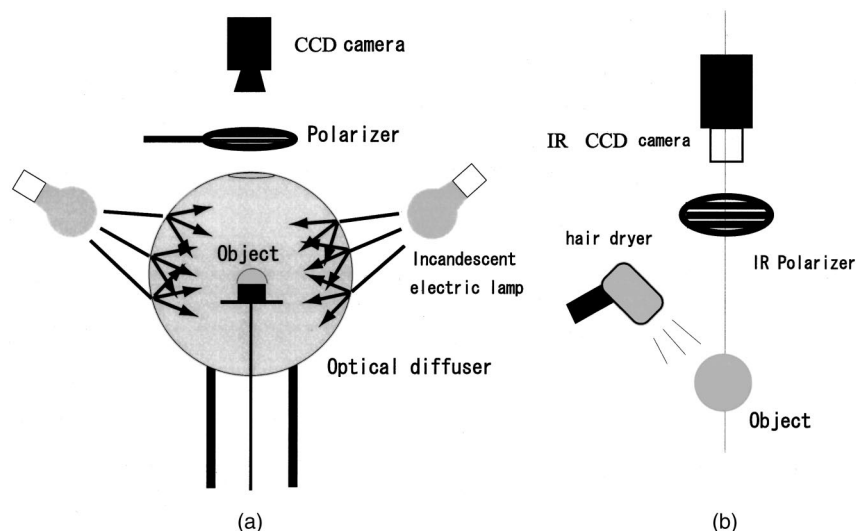


Fig. 6. Experimental setup: (a) apparatus for visible light, (b) apparatus for infrared light.

are the same, it is necessary to illuminate an object from all directions in order to observe surface reflections over the entire object surface.

We use three 300-W incandescent light bulbs as the point sources, located circularly 120 deg apart. The spherical diffuser is made of plastic, and its diameter is 40 cm. The object, as mentioned above, is located at the center of the sphere, and is illuminated by this spherical diffuser, which functions as an unpolarized spherical light source. The object is observed through a small hole at the top of the sphere by a black-and-white CCD camera. A polarization filter is mounted between the hole and the camera.

B. Apparatus for Infrared Light Measurement

Figure 6(b) shows the apparatus for use with infrared light. Given that the infrared light is thermal radiation from a body and is not a reflection component, we do not use an additional light source. Any object emits infrared light. However, at room temperature the amount of infrared light emitted from the object at 3–5 μm is relatively small, and contains infrared light emitted from the air. This makes the measurement of I_{max} and I_{min} very sensitive to noise. Thus, we increase the temperature of the object to 30–40° C and subtract that from that of the air to obtain the amount of infrared light emitted solely by the object.

To increase the temperature of the object, we use a hair dryer to blow heated air over it. We also employ an infrared filter and an IR-CCD camera at 3–5 μm . Our IR-CCD camera measures the intensity and converts it to a temperature. To determine the polarization ratio, we convert the measured temperature back into intensity, using Eq. (6).

C. Experimental Method

Because a transparent object reflects and transmits light, the observed intensity in visible light measurement is the combination of the light reflected at the surface and the light transmitted from behind the object. We set the ob-

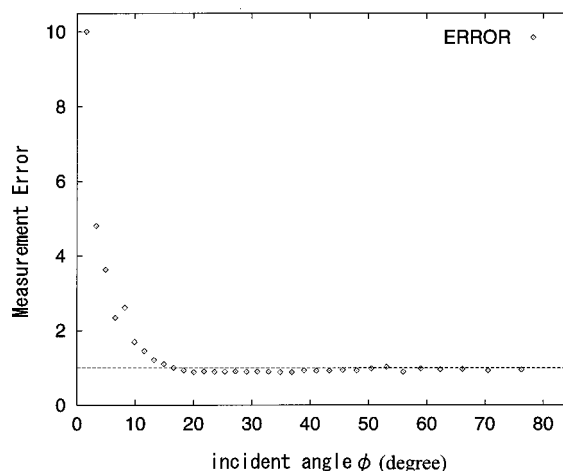


Fig. 7. Error characteristics of the spherical object.

ject on a black pipe to block the light from behind the object. We should observe only the light reflected directly from the surface and originating from the light source, though the light reflects and transmits randomly through the object. The shape of the object is not known *a priori*, so we cannot estimate such internal reflection exactly. We assume that any component of the light not directly reflected from the surface is relatively small and that we observe only the light reflected directly from the surface.

In visible light measurement, by rotating a polarization filter we obtain a sequence of images of an object. We measure from 0–180 deg at 5-deg intervals. From this process we obtain 36 images.

At each pixel of each of the 36 images, we observe variance of intensity and determine the maximum and minimum intensities, I_{max} and I_{min} . Because those measurements occur at 5-deg intervals, it is difficult to obtain the exact maximum and minimum values. By using the non-linear least-squares minimization, we fit a sinusoidal curve to those measurements and then determine the maximum and minimum values. From those values, we determine two possible surface orientations from Eqs. (4) and (5).

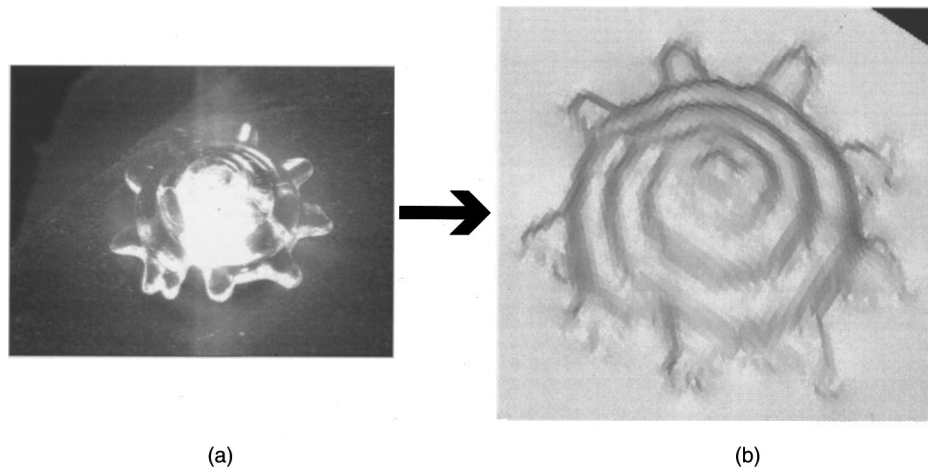


Fig. 8. Derived shape of shellfish-shaped object: (a) acrylic object, (b) derived image.

For the infrared measurement, we heat the object to a temperature of 30–40 °C by using the hair dryer for a certain period. Once equilibrium in the heat exchange is achieved, we use the same procedure, rotating the polarization filters and obtaining a sequence of images, as we did in the visible light measurement. Here the maximum and minimum correspond to T_{\max} and T_{\min} ; we convert them to I_{\max} and I_{\min} as appropriate and then obtain the polarization degree.

In the third step, we compare the measurements in infrared and visible light at each pixel. For alignment, we use two calibration points around the object; by extracting these two points in both image sequences, we can align the two measurements. At each pixel, measurement in visible light provides two solutions. Then from the measurement of the degree of polarization in the infrared, we can choose one of the solutions. Thus we determine whether the measured degree of polarization in infrared light is smaller or larger than the degree of polarization in visible light at the Brewster angle, ρ_{IR}^* .

D. Experiments Using a Spherical Object

To determine the accuracy of the system, we use an acrylic sphere having a refractive index of 1.5 and a diameter of 5 cm. Figure 7 shows the error characteristics from the observed measurement. The horizontal axis is the emitting (incident) angle, and the vertical axis denotes the measurement errors. In the figure, the dashed horizontal line denotes the case without any measurement errors.

From this experiment, the measurement error is small except in the area of small angles, and we can achieve high accuracy in our measurements.

One of the reasons for the relatively noisy data near smaller angles is that the spherical diffuser has a hole in its top portion, so the object does not receive light from that area. Another reason is that the derivative of the degree of polarization is close to zero where the incident angle is near 0°, and is less stable for determining the incident angle from the degree of polarization.

E. Experiments Using a Shellfish-Shaped Object

To demonstrate the applicability of our system to an object of general shape, we determined the shape of the ob-

ject shown in Fig. 8(a). The shellfish-shaped object is made of acrylic, and its refractive index is 1.5. Figure 8(b) shows the obtained shape of the object. Here the system provides the distribution of surface orientations. From this obtained distribution, a relaxation algorithm²³ converts the orientation distribution into a shape corresponding to that of the object.

Figure 8(b) recovers the original shape. Notably, the regions of steeper angles (i.e., those larger than the Brewster angle) provide better recovery results. At the boundary, the shape is a bit noisy; the polarization ratio there is almost zero, and it is difficult to determine this value.

4. CONCLUSIONS

This paper proposes a method for determining the shape of a transparent object by using the polarization of reflected and emitted light. Surface orientations are determined by using the polarizations in visible light. Because an algorithm that uses visible light results in ambiguities, polarization in the infrared is then employed. The thermal radiation, which also has characteristics of polarization, can be observed as infrared light. This polarization is a one-valued function; measuring polarization ratio in the infrared provides the emitting angle. However, the ratio is relatively low, and in some cases it is difficult to determine the ratio precisely. Thus we propose to use polarization in both visible and infrared light.

We have implemented the proposed method and demonstrated its ability to determine the shape of a transparent object. First, by using a spherical acrylic object, we determined the accuracy of the method in the visible light region and demonstrated its effectiveness. Then, using an object of general shape, we demonstrated the ability of the system to determine the shapes of complex objects.

Corresponding author Daisuke Miyazaki receives e-mail at miyazaki@cvl.iis.u-tokyo.ac.jp.

REFERENCES

1. K. Ikeuchi, "Determining surface orientations of specular surfaces by using the photometric stereo method," *IEEE Trans. Pattern Anal. Mach. Intell.* **3**, 661–669 (1981).

2. S. K. Nayar, K. Ikeuchi, and T. Kanade, "Determining shape and reflectance of hybrid surface by photometric sampling," *IEEE Trans. Rob. Autom.* **6**, 418–431 (1990).
3. Y. Sato, M. D. Wheeler, and K. Ikeuchi, "Object shape and reflectance modeling from observation," in *Proceedings of SIGGRAPH 97* (Addison-Wesley, Boston, Mass., 1997), pp. 379–387.
4. M. Oren and S. K. Nayar, "A theory of specular surface geometry," *Int. J. Comput. Vis.* **24**, 105–124 (1997).
5. K. Koshikawa, "A polarimetric approach to shape understanding of glossy objects," in *Proceedings of the International Joint Conference on Artificial Intelligence* (Morgan Kaufmann, Los Altos, Calif., 1979), pp. 493–495.
6. K. Koshikawa and Y. Shirai, "A model-based recognition of glossy objects using their polarimetric properties," *Adv. Robot.* **2**, 137–147 (1987).
7. L. B. Wolff, "Polarization-based material classification from specular reflection," *IEEE Trans. Pattern Anal. Mach. Intell.* **12**, 1059–1071 (1990).
8. L. B. Wolff and T. E. Boult, "Constraining object features using a polarization reflectance model," *IEEE Trans. Pattern Anal. Mach. Intell.* **13**, 635–657 (1991).
9. S. Rahmann, "Polarization images: a geometric interpretation of shape analysis," in *Proceedings of the International Conference on Pattern Recognition* (IEEE Computer Society, Los Alamitos, Calif., 2000), pp. 542–546.
10. D. L. Jordan and G. D. Lewis, "Measurements of the effect of surface roughness on the polarization state of thermally emitted radiation," *Opt. Lett.* **19**, 692–694 (1994).
11. D. L. Jordan, G. D. Lewis, and E. Jakeman, "Emission polarization of roughened glass and aluminum surfaces," *Appl. Opt.* **35**, 3583–3590 (1996).
12. L. B. Wolff, A. Lundberg, and R. Tang, "Image understanding from thermal emission polarization," in *Proceedings of the IEEE Conference on Computer Vision and Pattern Recognition* (IEEE Computer Society, Los Alamitos Calif., 1998), pp. 625–631.
13. R. Szeliski, S. Avidan, and P. Anandan, "Layer extraction from multiple images containing reflections and transparency," in *Proceedings of the IEEE Conference on Computer Vision and Pattern Recognition* (IEEE Computer Society, Los Alamitos, Calif., 2000), pp. 246–253.
14. Y. Schechner, J. Shamir, and N. Kiryuati, "Polarization-based decorrelation of transparent layers: the inclination angle of an invisible surface," in *Proceedings of the IEEE International Conference on Computer Vision* (IEEE Computer Society, Los Alamitos, Calif., 1999), pp. 814–819.
15. D. E. Zongker, D. M. Warner, B. Curless, and D. H. Salesin, "Environmental matting and compositing," in *Proceedings of SIGGRAPH 99* (Addison-Wesley, Boston, Mass., 1999), pp. 205–214.
16. M. Saito, Y. Sato, K. Ikeuchi, and H. Kashiwagi, "Measurement of surface orientations of transparent objects using polarization in highlight," in *Proceedings of the IEEE Conference on Computer Vision and Pattern Recognition* (IEEE Computer Society, Los Alamitos, Calif., 1999), pp. 381–386.
17. M. Saito, Y. Sato, K. Ikeuchi, and H. Kashiwagi, "Measurement of surface orientations of transparent objects by use of polarization in highlight," *J. Opt. Soc. Am. A* **16**, 2286–2293 (1999).
18. K. E. Torrance and E. M. Sparrow, "Theory for off-specular reflection from roughened surfaces," *J. Opt. Soc. Am.* **57**, 1105–1114 (1967).
19. M. Born and E. Wolf, *Principles of Optics* (Pergamon, New York, 1959).
20. F. E. Nicodemus, "Directional reflectance and emissivity of an opaque surface," *Appl. Opt.* **4**, 767–773 (1965).
21. F. E. Nicodemus, "Reflectance nomenclature and directional reflectance and emissivity," *Appl. Opt.* **9**, 1474–1475 (1970).
22. O. Sandus, "A review of emission polarization," *Appl. Opt.* **4**, 1634–1642 (1965).
23. K. Ikeuchi, "Reconstructing a depth map from intensity maps," in *Proceedings of the International Conference on Pattern Recognition* (IEEE Computer Society, Los Alamitos, Calif., 1984), pp. 736–738.